ADVANCED FUNCTIONAL MATERIALS
www.afm-journal.de

Two-Dimensional Transition Metal Dichalcogenides in Biosystems

Kourosh Kalantar-zadeh, Jian Zhen Ou, Torben Daeneke, Michael S. Strano, Martin Pumera,* and Sally L. Gras*

The intriguing properties of two-dimensional transition metal dichalcogenides (2D TMDCs) have led to a significant body of fundamental research and rapid uptake of these materials in many applications. Specifically, 2D TMDCs have shown great potential in biological systems due to their tunable electronic characteristics, unique optical properties, stability in aqueous environments, large surface area that can be manipulated and functionalized as well as an intercalatable layered structure, and low levels of toxicity. Here, the characteristics and use of 2D TMDCs for biological applications are reviewed and future possibilities for these materials in biological systems are outlined.

1. Introduction

Two-dimensional transition metal dichalcogenides (2D TMDCs), which are planar crystals made of one or a limited number of TMDC unit cells, possess rich electronic, optical, mechanical, and chemical properties.[1–6] Single-layered TMDCs are described by the formula MX_2, where M is the transition metal from groups 4–10 of the periodic table and X is a chalcogen (S, Se, or Te) (**Figure 1**a). Common polymorphs of TMDCs include 1T, 2H, and 3R crystal phases (Figure 1a).[7] Different combinations of transition metals and chalcogens as well as their various arrangements in the 2D crystals lead to a substantial range of properties,[7,8] making these materials suitable for applications in biological systems such as drug delivery, therapeutics, bioimaging, tissue engineering and biosensing as well as many others.[9–21]

Diverse techniques are available for synthesising 2D TMDCs[4,8,22] and as such, it is always possible to adopt the right method suitable for almost any biosystem. The surface of 2D TMDCs has no unpaired valence electrons, or so called dangling bonds, leading to high stability in liquid and air, facilitating their incorporation in biosystems.[23] In their nanoflake morphology, 2D TMDC can feature either metallic or chalcogen edge terminations. Both basal surfaces and prismatic edges can be readily functionalized via established methods to facilitate bio reactions, and to target specific biomaterials.[24] Depending on the intended bio application, the number of layers and lateral dimensions of 2D TMDCs can be tuned in order to produce different vibrational or optical properties.[3,4,25,26] The large surface areas offered by 2D TMDCs can be used for enhancing biological interactions. Upon such interactions, their whole bulk can be affected as the plane thickness is generally less than the Debye length.[27] 2D TMDC energy band diagram can be efficiently engineered. Their electronics can be adjusted ranging from insulating to fully conducting in order to make them suitable for any bio processes and templates. Additionally, the photoluminescence and plasmonic properties of these materials allow optical observations within cells and biosensing.

2D TMDCs have been shown to induce fewer cytotoxic responses in cells than many other nanostructures,[6,28] making these materials potentially valuable for biological applications in which health and safety is of paramount importance. Cellular viability appears largely unaltered by the uptake of 2D TMDCs, and they have large surface areas, so they can subsequently act as nano carriers. A key feature of 2D TMDCs is their ability to intercalate ions and organic molecules that facilitate sensing or inducing cellular responses.[17,26] 2D TMDCs have been used for constructing biosensors with high quality conductormetric and field effect based sensing[29] as well as for effective bioimaging.[3,4,25,26] They have been effectively used for photothermal therapeutics.[15,30,31] Additionally, the mechanical properties of 2D TMDCs can be used for establishing desirable frameworks for tissue engineering and for establishing atomically thin acoustic transducers.[32,33]

Here, we highlight and analyse the characteristics of 2D TMDCs and describe methods for synthesising, functionalizing

Prof. K. Kalantar-zadeh, Dr. J. Z. Ou, Dr. T. Daeneke
School of Electrical and Computer Engineering
RMIT University
Melbourne, Victoria 3001, Australia
E-mail: kourosh.kalantar@rmit.edu.au
Prof. M. S. Strano
Department of Chemical Engineering
Massachusetts Institute of Technology
Cambridge, MA 02139, USA
Prof. M. Pumera
School of Physical & Mathematical Sciences
Nanyang Technological University
Singapore 637371, Singapore
E-mail: pumera@ntu.edu.sg
Prof. S. L. Gras
Department of Chemical and Biomolecular Engineering
The University of Melbourne
Parkville, Victoria 3010, Australia

DOI: 10.1002/adfm.201500891

and incorporating these materials into biological systems. We also outline possible future research directions for 2D TMDCs in biological systems.

2. Electronic Band Structures and Vibrational Characteristics

The electronic band structure and the charge properties of TMDCs are governed by the *d*-electron count and coordination environment of the transition metal atoms.[7] The four electrons from the metal atoms fill the bonding states around them and the surfaces of the layers are terminated by the chalcogen lone-pair electrons, resulting in no dangling bonds, which makes the layers chemically inert. Some TMDCs such as Mo and W dichalcogenide compounds show indirect-to-direct bandgap transition when exfoliated from many layered bulk crystal to a single layer (Figure 1b).[3,34] In contrast, graphene has no bandgap and special manipulations such as lateral dimension narrowing[35] or layer stacking are needed to open the gap.[36]

In semiconducting 2D TMDC, the bulk crystal has a valence band maximum (VBM) at Γ and a conduction band minimum (CBM) in mid of Γ–K. Single layers of the same materials are direct-band gap, in which VBM and CBM coincide at K. Spin and valley coupling are observed in monolayers of group 6 TMDCs.[37] The electronic band structure can also be a strong function of the lateral dimensions.[17,26] Further information regarding the crystal phases and electronics of 2D TMDCs can be found in other review papers.[4,7] The changes in the band structures allow designing these 2D systems ranging from insulating to highly conductive, which are especially important in biosensing and tissue engineering.[12] The emergence of direct bandgap, and hence fluorescence effect, is also beneficial for many biosensing and bioimaging applications.[38,39] The electronics of semiconducting 2D TMDCs allow remarkable on/off ratios with acceptable carrier mobilities for establishing field effect transistors (FETs) for biosensing (Figure 1c,d).[6] Overall, the optical and electronic properties of the biosystems based on 2D TMDCs depend on the bandgap energy and the location of the band edges of these materials. Figure 1e presents the energy level diagram of selected 2D TMDCs.[40–42] The diversity of band gap sizes and band positions provides great opportunities to choose the 2D TMDCs with desired properties for any specific bio application. It is important to consider that indirect and small band-gap of transition metal dichalcogenide compounds of Ti, V, Ta, and Cr result in their near metallic behaviors.[43]

In 2D TMDCs, the concentration and mobility of the charges depend on the choice of the transition metal and chalcogenide which govern the properties of these materials, such as charge transfer to their bio environments and affinity to bio components.[4,41] It is also important to consider that electrons in 2D TMDCs are massive, while in graphene they are massless like.[44]

It is essential to know that changes in the lateral dimensions of 2D TMDCs can completely alter their electronic band structure and hence optical properties. Reducing the lateral dimensions of semiconducting 2D TMDCs introduces strong photoluminescence (PL) peaks which are blue shifted and broad in nature (Figure 1g).[17,26] Very interestingly, even metallic 2D TMDCs show similar broad PL responses upon reduction of their lateral dimensions.[45] This effect is likely due to the spatial quantum confinement effect of the electron clouds analogous to observations in other metallic nanoparticles. The effect is particularly useful in optical biosensing which will be described later.

2D TMDCs have strong infrared vibrational characteristics, which are the function of the number of layers (Figure 1f), added mass to their surfaces and environmental effects (permittivity and charge). These properties, similar to those of graphene, are suitable for making a variety of biological and chemical observations via Raman and FTIR spectroscopies,[25] the former offering information at high spatial resolution. The added mass causes alterations in the Raman and FTIR peaks full width half height, while intercalation shifts the peaks.[26] Raman peak shifts are also important in determining the number of layers. While in grapheme, the ratio of these peaks alters with the number of layers,[46] in most 2D TMDs a subtle shift takes place, when the thickness is changed.[25]

3. Synthesis Techniques

Many methods have been developed for the synthesis and exfoliation of 2D TMDCs. Direct mechanical exfoliation techniques

Kourosh Kalantar-zadeh is a full Professor and the Director of the Centre for Advanced Electronics and Sensors (CADES) at RMIT University, Australia. He received his B.Sc. (1993) and M.Sc. (1997) degrees from Sharif University of Technology and Tehran University, respectively, and his Ph.D. from RMIT University (2001). Prof. Kalantar-zadeh's research interests are diverse including chemical and biochemical sensors, nanotechnology, materials sciences, electronic circuits, gastroenterology and microfluidics.

Martin Pumera is a faculty member at Nanyang Technological University, Singapore since 2010. After receiving his Ph.D. in 2001 and two postdoctoral stays (USA and Spain), he joined the NIMS, Japan in 2006, where held a tenured position. Prof. Pumera has broad interests in nanomaterials and microsystems, in the specific areas of nanomotors and nanorobots, nanotoxicity, electrochemistry and synthetic chemistry of 2D nanomaterials

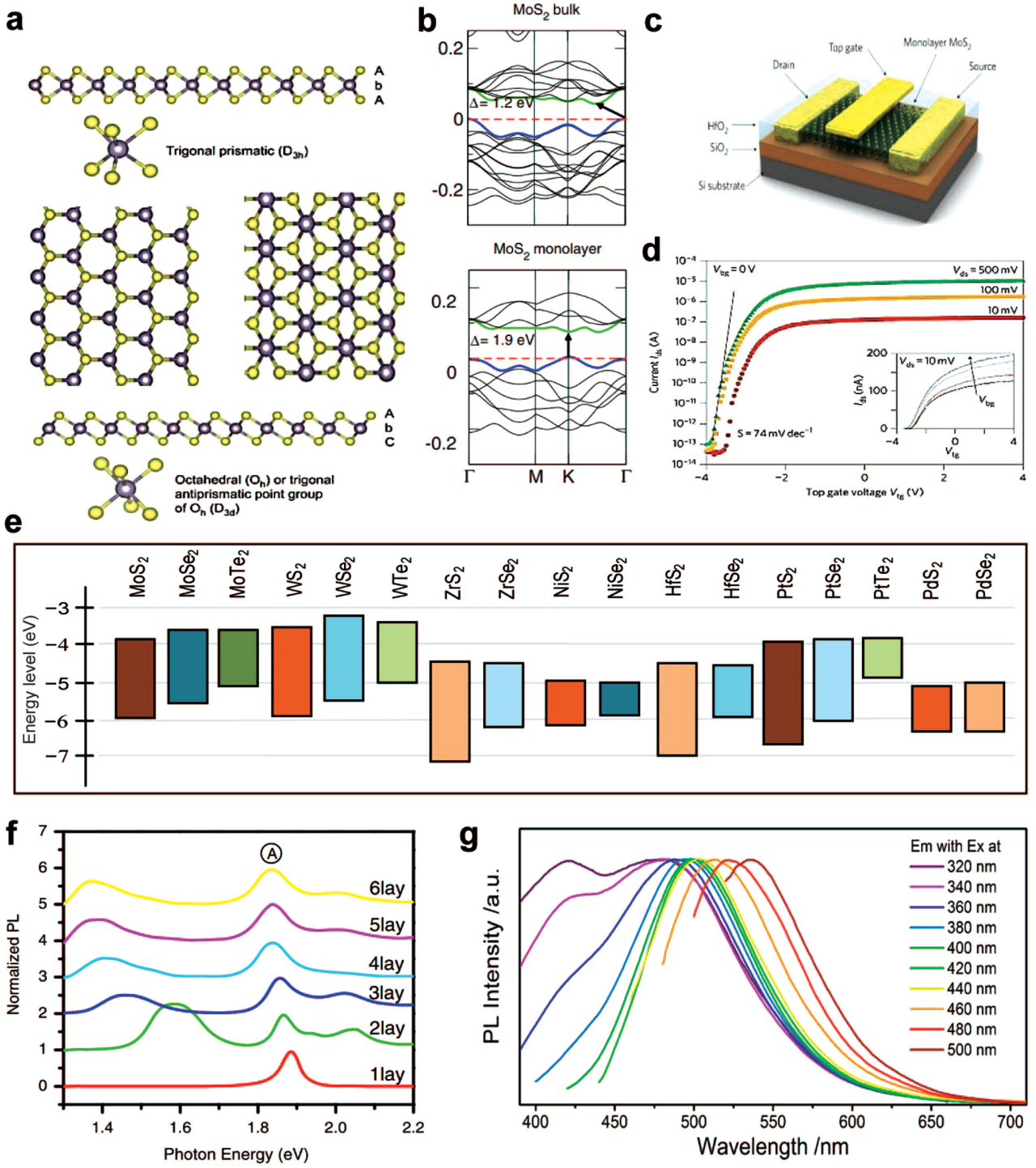

Figure 1. Selected characteristics of 2D MoS_2 as a typical 2D TMDCs. a) Chemical structure of 2H and 1T polytypes of one-layer TMDC, where M is a transition element and X is a chalcogen. Reproduced with permission.[7] Copyright 2015, Nature Publishing Group. b) Band structure of bulk and single-layer MoS_2 as calculated using density functional theory. Reproduced with permission.[125] Copyright 2015, American Physical Society. c) Schematic illustration shows a top-gated single layer MoS_2 FET. d) Semi-log transfer characteristics of such a FET with a 30 nm thick hafnia dielectric. The low subthreshold swing, low operating voltage, and high on/off ratio result from enhanced gate coupling. Reproduced with permission.[6] Copyright 2015, Nature Publishing Group. e) Energy level diagram of selected 2D TMDCs. Reproduced with permission.[40–42] Copyright 2015, American Chemical Society. f) Photoluminescence spectra of thin layers of MoS_2 for number of layers from 1 to 6. The spectra are normalized by the intensity of peak A. Reproduced with permission.[3] American Physical Society. g) Photoluminescence spectra of 2D MoS_2 suspended nanoflakes under excitation wavelengths of 320–500 nm. Reproduced with permission.[19] Copyright 2015, American Chemical Society.

generally result in the highest-quality monolayers,[47] but are low in yield and form nanoflakes that land randomly on substrates. A variety of gas/vapor synthesis methods are suitable for wafer scale growth of 2D TMDCs.[48,49] Some start by placing a very thin layer of organic or inorganic precursor of the TMDC followed by annealing and chalcogenisation at high temperatures.[50] Chemical vapor deposition (CVD) using chalcogen and transition metal containing vapors can also be employed to obtain large stratified MX_2 crystals for mechanical exfoliation,[51] as well the direct growth of 2D TMDCs onto selected substrates. For the latter, the present challenge is to obtain high crystallinity and homogenousity over the entire substrate.

Liquid exfoliation synthesis methods are suitable for obtaining suspensions of 2D flakes compatible with many biological systems. One of the most high yielding liquid exfoliation methods involves ultrasound-promoted hydration of lithium-intercalated compounds,[52] however, some serious challenges remain including the hazardous nature and long duration of this process. It has also been shown that lithiation can be electrochemically applied, avoiding the hazardous chemical exfoliation procedures.[53] Since 2011, Colman et al. have reported a series of liquid phase exfoliation methods that rely on the shear forces in chaotic liquid flow to exfoliate stratified TMDCs,[54–56] assisted by surfactants or organic solvents. Such methods can tailor the suspensions solvent environment to meet the biological requirements of the proposed application. There is a quest for developing green methods for liquid exfoliations to achieve the highest compatibility with biosystems. Very recently bovine serum albumin (BSA) has been shown to be an effective exfoliating agent that can also function as a stabilizing agent while improving biocompatibility.[57] The use of complimentary exfoliating liquid is also beneficial in tailoring the grinding and exfoliation processes.[58,59]

Vapor phase procedures generally result in clean 2D TMDC surfaces. In contrast, liquid phase processes that involve ionic or organic compounds may leave residues on the resulting 2D TMDC flakes. Due to high surface areas and the large van der Waals forces, surface cleaning is always a challenge. Several centrifuge steps can assist in removing remnants. Non-polar hydrocarbon solvents, such as hexane, have also commonly been used for cleaning. Annealing may also help removing low boiling point residues, however, annealing temperatures above 300 °C can potentially deteriorate the integrity of 2D TMDCs.[59] Understanding the biological impact of residues left on the surface is critical for surface functionalization and intersections with biological components.

4. Functionalization

Functionalization of 2D TMDCs is an important process for facilitating the interactions between these materials and bio components. Non-specific functionalizations have so far been the most widely used process for incorporating 2D TMDCs into biosystems. The large surface areas of 2D TMDCs allow the effective and fairly strong adsorption of organic/inorganic components via van der Waals and/or ionic forces on the surface of these materials.

The specific functionalization process typically involves the modification of either basal plane or the edges, kinks and corner atoms in 2D TMDCs. The basal plane surface can be functionalized using silane based chemistry, which is commonly employed for modifying oxides and chalcogenides surfaces.[60] As theoretically demonstrated, this type of functionalization is predicted to dramatically change the electronic band structure of 2D TMDCs.[61] Covalently bound amide and methyl moieties have been grafted onto sulphur- and selenium- based metallic 2D TMDCs (**Figure 2**a),[62] changing it from metallic into a semiconducting phase.

The edges and kinks (lattice defects) in 2D TMDCs are terminated by either metal or chalcogen atoms, depending on the conditions of synthesis.[7,63] The exposed metallic atoms can be utilised to incorporate functional groups such as hydroxyls and thiols, which are essential in many well-established bio functionalization procedures. Thiolation (Figure 2b) and the formation of disulphide bonds have been successfully used for functionalizing 2D TMDC flakes with organic compounds and the immobolisation of biological molecules via metallic edges and defects.[64,65] Similarly organic oxoacids of sulphur can be used for functionalizing 2D TMDCs in order to bind proteins and carbohydrates, while they may act themselves as catalysts or intermediates for bio interactions. Many other methods such as in situ reduction of metal ions, esterfication, ring-opening polymerisation and free radical polymerisation can also be used.

Functionalization also plays important roles in stabilising 2D TMDCs suspensions in ionic solutions such as phosphate buffered salines, which are essential for many biological applications. Thiolated molecules with tailored ends provide extra stability.[65] Additionally, there are suggestions that more complex systems such as lipoic acid conjugated PEG (LA-PEG) can further improve colloid stability.[15]

Extensive studies on catalytic systems have revealed that the chemistry of defects and edge sites is fundamentally different from the chemistry of the basal planes. For example, it has been suggested that the rim sites of 2D TMDCs are responsible for hydrogenation reactions and the edge sites for sulphur removal processes.[52] While these effects in 2D TMDCs are not as strong as in their metallic nanoparticle counterparts, their presence can produce effects which are important in biodegradation processes for the removal of bacterial and viral impurities. 2D TMDCs generally show strong resistance to catalytic poisoning,[66] and are stable in photo activated reactions.[67] These properties are an important asset for biosensing and tissue engineering, potentially reducing biofouling.

5. Intercalation

When biologically important charged particles or bio components are brought within the vicinity of 2D TMDCs, which are made of more than two layers, a portion of these materials is adsorbed onto the surface and a fraction can be intercalated into the TMDC crystal (reversibly included into the layered crystal).[52] Guest molecules can be incorporated by ionic and non-ionic interaction processes[52] or by exfoliation–restacking,[60] where molecules are incorporated during the restacking of the exfoliated 2D sheets (Figure 2c).

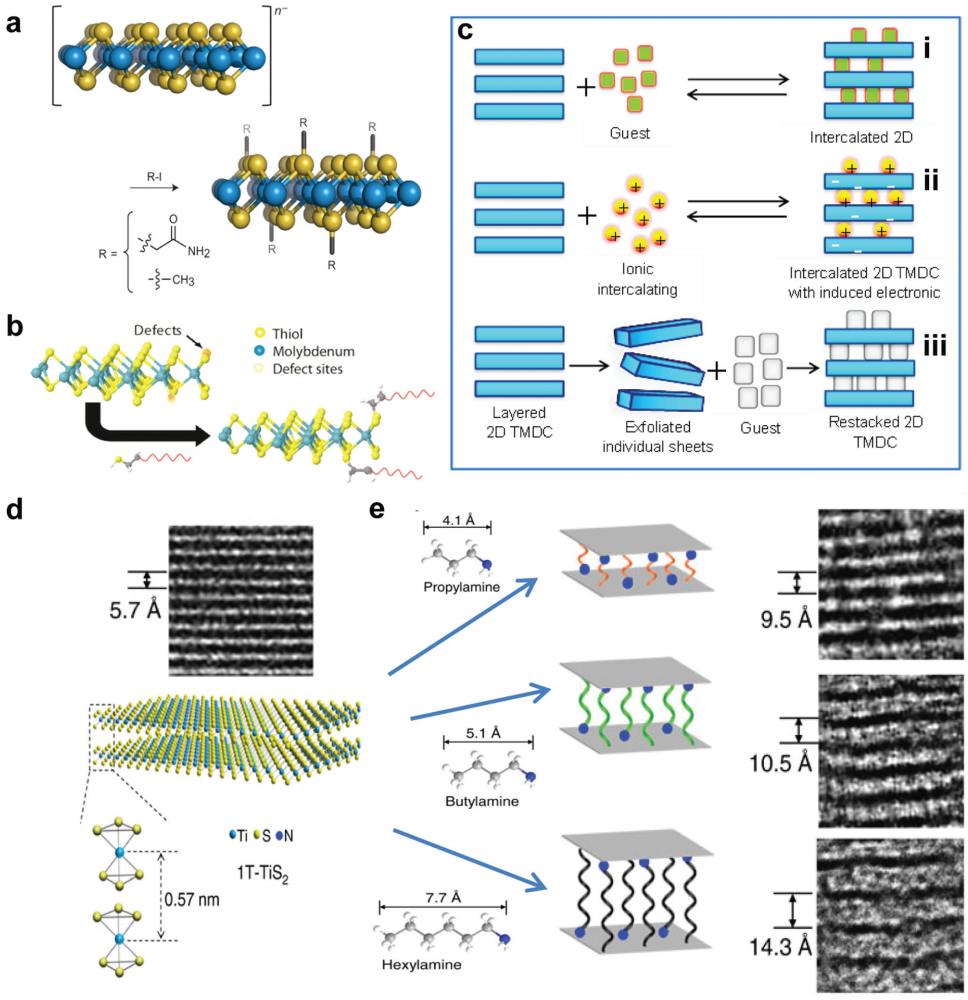

Figure 2. Functionalization and intercalation of 2D TMDCs. Schematic diagrams depicting: a) Covalent functionalization of metallic 1T phase nanosheets using a 2-iodoacetamide or iodomethane (R-I) solution. Reproduced with permission.[62] Copyright 2015, Nature Publishing Group. b) Thiols and other suitable functional groups bond onto defects, Reproduced with permission.[65] Copyright 2015, American Chemical Society. c) Intercalation and surface absorption of guest particles (non-ionic and ionic) between 2D TMDC layers and onto the surface, respectively: i) general intercalation concept, ii) charged particles intercalation, and iii) exfoliation and restacking processes. Size-dependent interlayer expansion of multilayer TiS_2 after intercalation. d) Visualisation of 2D TiS_2 using ball and stick model and the side view of such layers obtained using high resolution transmission electron microscopy (HRTEM). e) Schematic illustration of interlayer distance change of 2D TiS_2 by intercalating alkylamine as well as the side view of layers using HRTEM after intercalation using, propylamine, butylamine and hexylamine, respectively. Scale bar, 1 nm. Panels (c–e) are reproduced with permission.[68] Copyright 2015, American Chemical Society.

Intercalation may induce drastic changes in the electronics and transport properties of 2D TMDCs, tuning the optical and electrical properties. The intercalation processes of TMDCs are generally topotactic, in which interlaminar distances expand (Figure 2d,e) and can be tracked by measurements of spacing between the planes.[68] The intercalation process allows TMDCs to act as reservoirs of both electric charge and chemical species.[52]

When metal and hydrogen atoms are intercalated, electrons from these guest molecules are transferred to the lowest-lying unoccupied energy levels of the host 2D TMDCs defined by the transition metal *d* bands. The intercalation of H^+ and Li^+ ions has been the most studied due to their applications in energy research[69,70] but the importance of intercalation for biological systems has been largely ignored. Strong reductants, such as butyllithium, can naturally interact with TMDCs and intercalate them with their labile metal atoms.[52] Electrochemical,[26] microwave,[71,72] and other forms of energies can be provided to reduce the intercalation timescale from hours to several tens of seconds and also allow the use of less reactive charged sources.[52]

Intercalation techniques have been applied to different TMDCs including both metallic types such as NbS_2 and TiS_2 and semiconducting types including MoS_2, ZrS_2, and WSe_2.[68] Several organic molecules have been successfully intercalated into TMDCs to date. This includes a number of both saturated and conjugated polymers[71,73,74] that generate materials with interlaminar distances ranging from 1.1 to 1.7 nm and amines intercalated within MoS_2,[75] although the geometrical topotactic model fails to some degree in the latter case as structural

changes may also occur.[52] Biological molecules such as peptides, proteins, aptamers and DNA have not yet been intercalated into 2D TMDCs. These experiments will require careful control of conditions including pH, temperature and a judicious use of energy to retain the biological activity of these molecules. The choice of intercalates with reference to the 2D TMDC is critical in the success of the process. Intercalates act as Lewis base donating electrons from their highest occupied molecular orbital (HOMO) to the TMDCs conduction band edge, which act as Lewis acid. Sufficient driving force is necessary to promote the intercalation reaction or otherwise external energy should be provided. The conduction band edges of group VI TMDCs (e.g., MoS_2, $MoSe_2$, $MoTe_2$, WS_2, WSe_2, and WTe_2) is between −4.2 and −3.5 eV, which require strong reductants such as butlyl lithium for intercalation. Conversely, the conduction band edges of group IV TMCs (e.g., TiS_2, ZrS_2, $ZrSe_2$, HfS_2 and $HfSe_2$) are in between −6.0 to −5.5 eV, which are more readily intercalated using weaker Lewis bases such as alkylamines.[68] A possible method to overcome the intercalation driving force is to implement tertiary compounds where the 2D TMDCs are pre-intercalated with a strong reductant and are then intercalated to a further extend with biomolecules and bio analytes. During the intercalation of organic compounds and biomolecules, the presence of charges within the layers or at the edges of 2D TMDCs may also be required to facilitate the process.

6. Optical Properties for Bioimaging and Cell Labelling

Optical biological imaging and cell labelling can be achieved with semiconducting 2D TMDCs that feature an electronic band structure that gives rise to strong excitonic and fluorescent (FL) properties in semiconducting 2D TMDCs. FL tagging can be used for tracing and sensing biological components and processes, which is described in the following sections. Visible excitonic peaks provide information regarding the dimensions of the flakes and their semiconducting properties,[76] which are important when tuning the cell uptake efficiency and for tissue engineering in general.

2D TMDCs can be functionalized and used for tagging and imaging, using a variety of conventional and near field optical microscopy techniques.[59] FL 2D TMDCs such as W, Mo, and Zr dichalcogenide compounds, can be efficiently used for imaging cell organs, targeting chemicals within and outside the cells as well as understanding processes such as FRET (Fosters resonance energy transfer). 2D TMDCs can also successfully bind to other flourophores and act as their vehicles or be used in sensing based on quenching and electron exchange processes. When small in the lateral dimensions (less than 50 nm), 2D TMDCs can be taken up by cells and used for high contrast cell labelling. This process may be targeted towards certain cells when the 2D TMDC is functionalized in order to display an appropriate cell specific ligand (**Figure 3**a).[19,31,77] Further optical applications include photothermal therapeutics where the thermal properties of both semiconducting and metallic TMDCs can be exploited (example presented in Figure 3b). Encouraging first results have been reported even though significant further investigations are required to understand the effect of energy band structure manipulations on the photothermal properties of 2D TMDCs. Further research could strive to targeted specific endocytic pathways using 2D TMDCs (as shown in Figure 3c), allowing localised delivery to subcellular organelles, as has been achieved for layered clays.[78] It is suggested that such activities should be more successful with of group IV 2D TMDCs (e.g., TiS_2, ZrS_2, and $ZrSe_2$) that show relatively low conduction band edges.

7. Toxicity

It is believed that 2D TMDCs have generally low toxicity in their bulk form. The toxicity of these materials has however been shown to be influenced by the parameters used in the production processes such as exfoliation conditions, as well as defect density and chemical composition. Consequently, it is still difficult to draw conclusions about the toxicity of the entire class of 2D TMDCs.

In vitro cell viability assays indicate differences between the cellular responses 2D TMDC materials induce. MTT and WST-8 assays, which measure cellular reduction, have been used for assessing the toxicity of semiconducting 2D TMDCs such as MoS_2, WS_2, and WSe_2.[28] While MoS_2 and $MoSe_2$ did not show an appreciable toxicity to lung cancer cells, WSe_2 induced significant toxicity, although this toxicity was still lower than that observed for graphene oxide and graphene. Readers can refer to studies such as presented in [79] for more detailed comparison of the toxicity of selected 2D TMDCs with graphene and graphene oxide. Studies on model mammalian cell lines show that decreasing the number of layers in 2D MoS_2 can increase the toxicity, which is attributed to the enhanced surface area, defects and edges.[80] There are also other studies using human pulmonary epithelial cells, demonstrating that the inhalation of 2D WS_2 and MoS_2 generates low health risk.[81]

Several in vivo toxicity tests have been conducted, including a study[15] where mice were injected with 2D MoS_2 functionalized with polyethylene glycol (PEG) at a concentration of ≈3.5 mg kg^{-1}. Treated mice were observed to have similar serum biochemistry assays and blood panel tests, suggesting no evidence of toxicity at this dose.

In contrast to studies that show the low cytotoxicity of 2D TMDCs for model mammalian cell lines, the work by Yang et al. demonstrated significant antibacterial activity of 2D MoS_2 sheets using *Escherichia coli*.[21] The 2D MoS_2 sheets were found to produce reactive oxygen species, causing oxidative stress that is not observed with graphene-based materials.[82] One reason for the different observed toxicity when compared to other in vitro and in vivo investigations,[15,28] can be associated to the different organisms tested.

Toxicity studies have also been conducted for metallic 2D TMDCs such as 2D TiS_2. They were examined in a mice model after the injection of PEG treated TiS_2. No toxic effect was observed after two months and organs remained intact.[83]

Given the wide ranging number of possible 2D TMDCs with different compositions, it is clear that more in vivo and in vitro studies are still required. The difference between the toxicity of semiconducting and metallic 2D TMDCs in their different electronic states should also be explored.

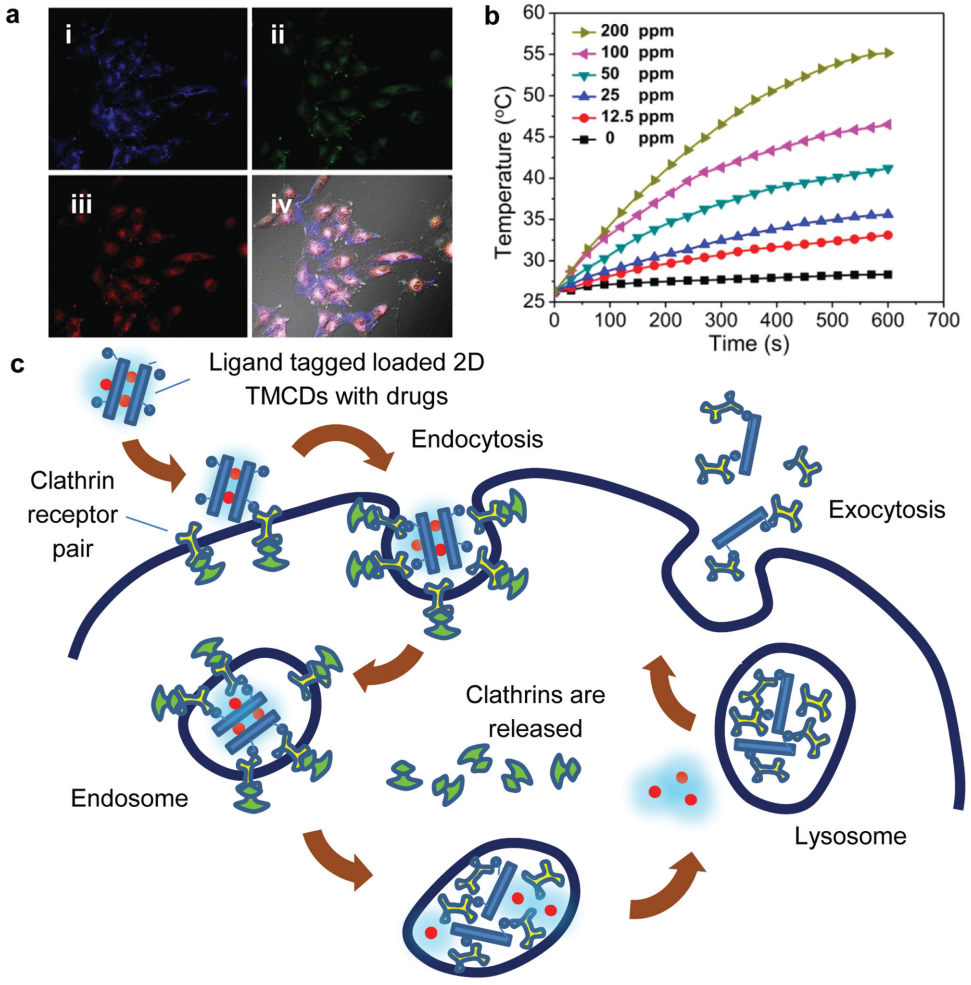

Figure 3. Drug delivery concept, cell imaging and photothermal properties of 2D TMDCs. a) FL images of lung cancer cells stained with 2D MoS_2 nanosheets of small lateral dimensions at excitation light sources of: i) UV (300–400 nm), ii) blue (400–500 nm), and iii) green (500–600 nm); iv) The overlay image of (i–iii) and a bright-field image, which shows specifically designed FL 2D MoS_2 nanosheets were taken up by the cytoplasm but did not penetrate the cell nuclei. The boundary between the cells, nuclei and cytoplasm is also clear. Reproduced with permission.[19] Copyright 2015, American Chemical Society. b) Photothermal profile of 2D MoS_2 nanosheets; the temperature increase of a water based 2D MoS_2 suspension with different concentrations of MoS_2 as a function of irradiation time. Reproduced with permission.[31] Copyright 2015, American Chemical Society. c) Schematic illustration of drug delivery concept, where layered 2D TMDCs are loaded with drugs and conjugated with a ligand allowing cellular uptake. The ligand on the 2D TMDC anchors to the receptor-clathrin pair facilitating clathrin mediated endocytosis. The loaded 2D TMDC enters the cell within a vesicle. In the later stages of transport the drug is released either from the surface or from within the layers. In the final step, ideally the emptied 2D TMDCs are externalised via extocytosis (under environmental changes such as pH lowering).

8. Delivery of Chemical Components in Biological Systems and Use as Therapeutic Agents

2D TMDCs have great potentials for pharmaceutical applications due to their many favorable properties including the ability to accommodate a large mass of drugs. They can act as nano carriers for controlled delivery of the molecules to targeted cells.[84] They also have photothermal and photosynthesis capabilities.[30,85]

Considering the surface adsorption (hydrophobic interactions) effect, the drug loading capability of 2D TMDCs has been shown to be remarkable. The highest reported drug loading ratios (weight ratios between the drug and 2D TMDCs) for a material such as the chemotherapy drug doxorubicin (DOX) in 2D MoS_2 systems is determined as ≈240%,[15] which is even higher than that of graphene oxide (≈150%).[84]

The near infra-red (NIR) absorbance of selected 2D TMDCs, such as MoS_2, is higher than that of other 2D materials such as graphene.[85] As a result, this NIR absorbance of 2D TMDCs makes these materials suitable for the photothermal ablation of diseases such as cancer. Relatively low concentrations of 2D MoS_2 suspensions (100 s of ppm) can reach temperatures ≥ 80 °C when subject to NIR radiation (≈800 nm, 0.8 W cm^{-2}) for several minutes,[30] allowing nearby cells to be destroyed.

The photothermal and drug carrying properties of 2D TMDCs can be combined to deliver NIR-triggered treatment with chemotherapeutic agents.[15,30,31] As a model, Yin et al.[31] injected 2D MoS_2 nanocarriers loaded with DOX to

NIR radiation triggered release of DOX and treat pancreatic cancer (**Figure 4**). These materials also featured a chitosan (CS) coating introduced during synthesis to increase stability and biocompatibility. Similarly, Liu, et al. functionalized 2D MoS_2 nanosheets with PEG to increase their stability and biocompatibility and attached folic acid to allow targeted entry to cancer cells.[15] The combined effect of NIR photoablation and DOX release from folic acid treated nanosheets, was synergistic and delayed tumour growth.[15] Similar approaches could be taken with other 2D TMDCs, as demonstrated with WS_2 and TiS_2.[83,86] These materials can be as efficient as 2D MoS_2 and also provide the same levels of biocompatibility. They can also be used for drug delivery and advantageously drugs can be comparatively easier intercalated into TiS_2 due to its more favorable energy levels. One issue that has yet to be established is the comparison between the metallic and semiconducting 2D TMDCs in NIR based treatments. Generally metallic nanoparticles are capable of generating localised enhanced plasmon effects, which help the electromagnetic wave absorption in the IR and visible regions.

2D TMDCs can also be utilised to deliver photosensitisers (PS) for photodynamic treatment of diseases, where photoenergy is used for generating singlet-oxygen species that induce cell death. 2D WS_2 has been employed to carry PS methylene blue, allowing for combined photothermal and photodynamic treatment.[86] In this case, NIR radiation regulates both oxidative stress caused by the 2D WS_2 nanoflakes and releases of the methylene blue photosensitive agent, illustrating the potential of 2D TMDCs to act as smart platforms for the controllable regulation of the process.[19]

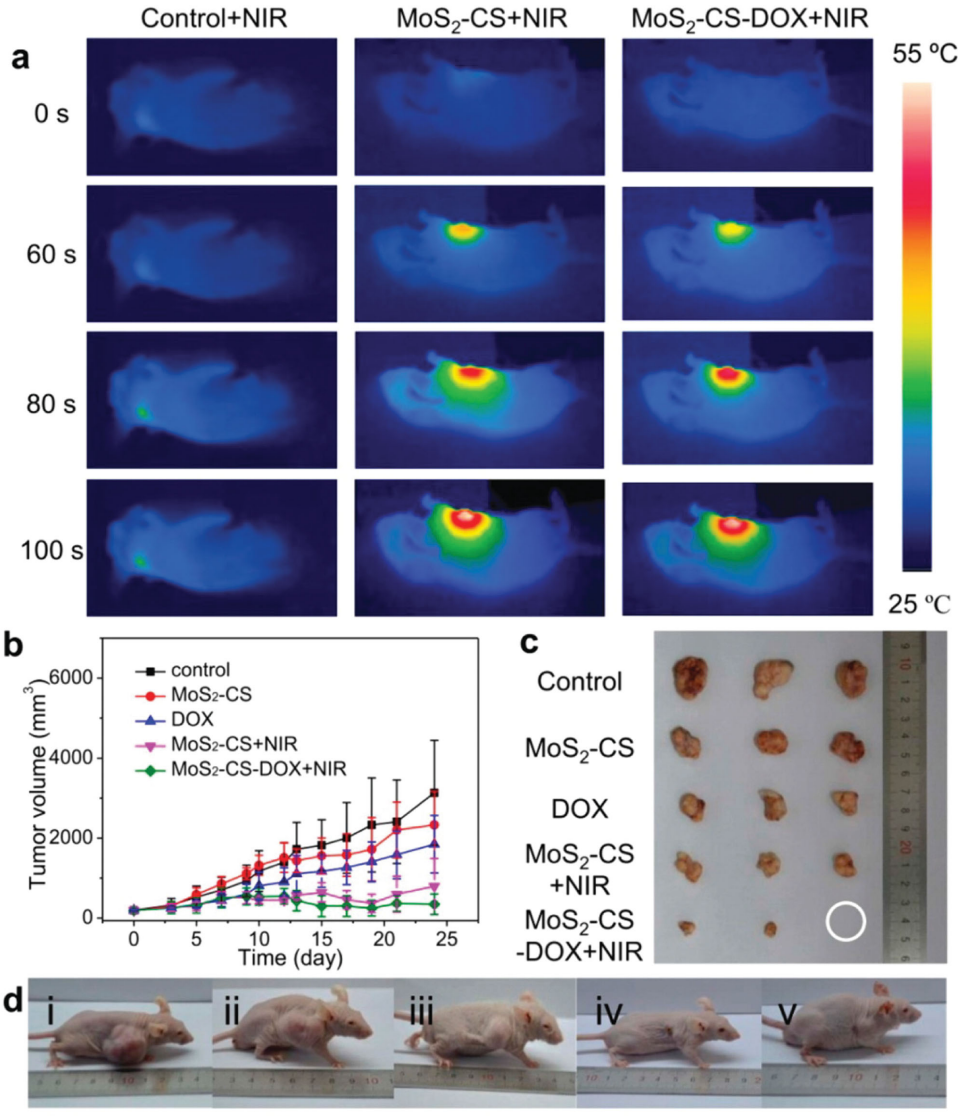

Figure 4. Photothermal delivery of chemotherapy drug DOX from 2D MoS_2 injected in pancreatic tumour bearing mice. a) Infrared thermal images of pancreatic tumour bearing mice injected with saline, 2D MoS_2-CS+NIR, and 2D MoS_2-CS-DOX+NIR laser. b) Tumour growth following the five treatments. c) Photographs of tumours following saline, 2D MoS_2-CS, DOX, 2D MoS_2- CS+NIR or 2D MoS_2-CS-DOX+NIR treatment. d) Photographs of the typical mice treated with i) saline+NIR, ii) 2D MoS_2-CS, iii) DOX, iv) 2D MoS_2-CS+NIR, or v) MoS_2-CS-DOX after observation for 24 days. Reproduced with permission.[31] Copyright 2015, American Chemical Society.

2D TMDCs can potentially increase solubility of drugs and enhance their life span. Advantageously in such applications, the uptake and release of drugs from FL 2D TMDCs can be traced. Other 2D TMDCs properties, such as lubrication, suggest they may find application as bases for cosmetic ingredients.

9. Bioimaging

Most 2D TMDCs can be used as contrast agents for bio-imaging since transition metal atoms such as W and Mo have a strong ability to attenuate X-rays. This effect is much stronger than that of carbon based materials including graphene.[85] So far, both 2D MoS_2 and WS_2 nanosheets have been used as promising contrast agents for X-ray computed tomographic (CT) imaging.[31,39,86] 2D TMDCs have also been implemented in photoacoustic tomography,[39] and they were found to be comparatively more efficient than their graphene based counterparts.[87] These functionalities are particularly useful when considered together with the possibility of 2D TDMC treatment discussed in the previous section, as it will potentially allow simultaneous diagnosis and treatment. Very recently, a report regarding decoration of 2D MoS_2 using self-assemble iron oxide nanoparticles has been presented.[88] Considering the magnetic properties of iron oxide, they could be used for magnetic resonance imaging (as well as photoacoustic tomography).[88] The same report also presented the possibility of positron emission tomography imaging using 2D MoS_2 onto which ^{64}Cu has been adsorbed.[88] It has been shown that PEG treated 2D TiS_2 can be efficiently used for photoacoustic tomography.[83] In addition, compounds of 2D MoS_2 and WS_2 have also been used for the same application.[89] More investigations are required to reveal the specific effects of metallic, semiconducting and compound 2D TMDCs on imaging processes and identify their advantages over one another.

10. Tissue Engineering

Another potential avenue for 2D TMDCs is in the creation of polymeric/2D TMDC composites for tissue engineering, although research activity in this area is only just beginning. The ability to functionalize 2D TMDC should assist biocompatibility, although the long term fate of 2D TMDC in vivo and potential for a foreign body reaction or inflammation is unknown.

2D TMDC can act as reinforcing agents within polymers; concentrations of 0.01–0.2% MoS_2 provide greater strength than single or multi-walled carbon nanotubes or graphene oxide plates on a weight for weight basis.[12] This reinforcement allows the development of materials that are light and durable. Properties such as material stiffness along the plane of the nanosheets, the ability to transfer mechanical loads from the polymer matrix and strong molecular interfaces between functionalized 2D TMDC materials and polymers are thought to lead to advantageous mechanical properties.[12,90] Dispersions need to be well controlled in order to prevent 2D TMDCs aggregation within the polymer matrix as large aggregates could cause slippages, leading to areas of concentrated stress and cracking.

Other possibilities for 2D TMDC composites include incorporation within porous scaffolds or combination with biomacromolecules commonly used for tissue engineering. Certainly greater study is required to understand the range of possible properties of nanocomposites containing 2D TMDCs. It is important to investigate the properties that metallic and semiconducting 2D TMDCs offer to tissue engineering as they feature inherently different electron transfer and charge transport characteristics. Also, it is expected that the metallic 2D TMDCs show stronger catalytic properties, and as result higher antibacterial capabilities, which should enhance the life time of the synthesised tissues if they used as bio implants.

11. Biosensing

Biosensing systems with 2D TMDCs feature in a significant number of recent publications. 2D TMDCs offer particular advantages for biosensing including: a high surface-to-volume ratio, versatility in functionalization, desirable optical properties in the visible wavelength range, electronic properties that range from insulating to metallic and layered structures that can accommodate ionic/organic compounds.[90]

Field effect and electrochemical transducing templates are currently the most investigated 2D TMDC device based sensors (**Figure 5**a–d). Field effect transducing templates can directly utilise the Bohr approximation equation to relate changes in charge or mass on the surface of the TMDCs to changes in the mobility of free carriers and subsequent alterations in transconductance.[2] These devices can operate label free and have been used to sense a variety of biochemical components including proteins and DNA.[18,38,91] Electrochemical based 2D TMDC devices are favorable for sensing bio related ionic species in redox systems. Graphene and graphene oxides have been successfully shown in field effect and electrochemical configurations for sensing biochemicals including a variety of proteins and DNA entities, and also chemical components with biological significance such as glucose, nicotinamide adenine dinucleotide (NADH), cholesterol, ascorbic acid, uric acid, dopamine and H_2O_2 as well as different gases and vapors.[92] Both metallic and semiconducting 2D TMDCs seem to be good choices for the working electrodes in electrochemical systems, specially the metallic systems can be advantageous for facilitating electron transfer between the biochemicals and the 2D layers, even more efficient than graphene, if their energy band diagrams are correctly selected against that of the target biomaterial. Semiconducting 2D TMDCs are useful for forming field effect biosensors, as their properties can be modulated using the immobilised biomaterials or electron exchange along their surfaces. However, metallic 2D TMDCs are logically less switchable, and hence cannot be electric field responsive.

To date, many examples of biosensors based on 2D TMDCs have been constructed. Wu et al. presented one of the first reports of such sensors, showing that a film of 2D MoS_2 has a fast electron transfer rate in selected redox systems.[93] They employed these devices for glucose and dopamine sensing. Electrochemical systems can also be used for DNA sensing in ppb ranges.[20,94] Like many other nano materials, the affinity of 2D TMDC towards single-stranded DNA is higher than for

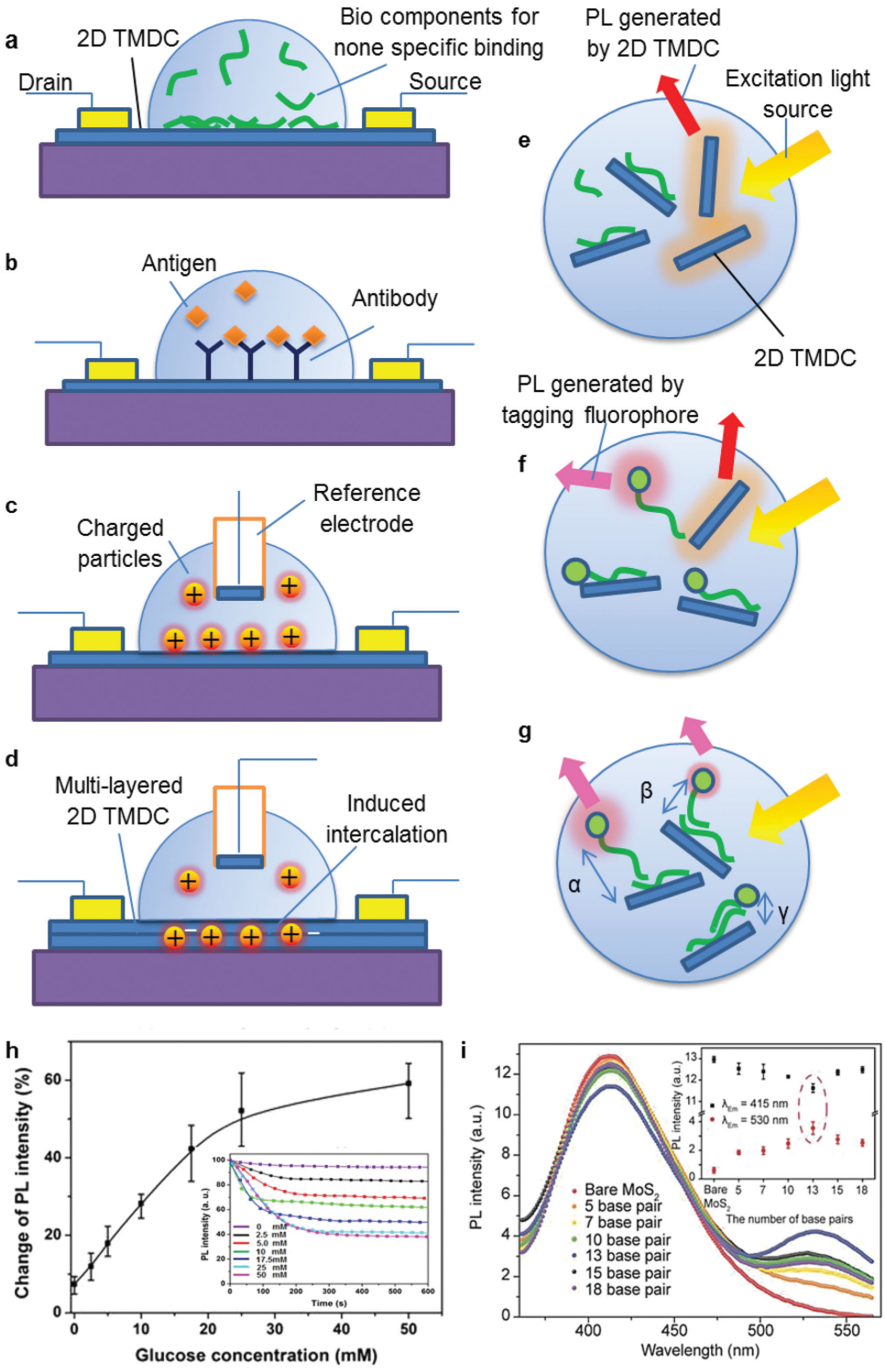

Figure 5. Biosensors utilising 2D TMDCs. Schematics illustrating different types of device based biosensing systems incorporating 2D TMDCs. FET based transducers respond to the added mass according to: a) Non-specific binding, b) Lock and key concept (antibody-antigen interaction in this example), c) With a reference electrode to produce the electrical double layer on 2D TMDCs and d) With a reference electrode, and multiple layer 2D TMDCs, to induce intercalation. Schematics illustrating different types of bio sensing systems based on 2D TMDCs suspensions: e) Non-specific immobilisation of bio components quenches the PL of 2D TMDCs, f) Fluorophore tagged bio components are themselves quenched after immobilisation and g) The possibility of observing FRET, both the PL of the tagged fluorophores and coupling between 2D TMDCs and flurophores are controlled by changing the distance between the 2D TMDCs and fluorophores (in the example $\alpha > \beta > \gamma$). h) Characterisation of the quasi 2D MoS_2–glucose oxidise system. The PL modulation of the system at an applied voltage of –1.5 V and at different glucose concentrations. Reproduced with permission.[17]

double-stranded DNA. Electrochemical 2D MoS_2 based devices have also been used for sensing H_2O_2, a by-product of many oxidative cellular reactions, in nM ranges.[95,96] Similar electronic based biosensors have also been shown for other 2D TMDCs.[97] It is predicted that 2D TMDCs with large free carrier mobilities such as 2D WSe_2 (as large as 500 $cm^2 V^{-1} s^{-1}$)[98] can establish the most sensitive and fastest response electronic biosensing templates, as they can show strong electrical modulation and also provide more facile paths for electron transfer.

The PL of semiconducting 2D TMDCs can be quenched (or possibly enhanced) upon interactions with biomolecules or the immobilisation of biomolecules on the TMDC surface (Figure 5e,f,h).[38] Such changes in PL have been associated with electronic energy transfer (EET), resonance energy transfer (RET) and electrostatic charges (Figure 5g,i).[10,99] However, general changes in the surface roughness can also play an important role in the alteration of PL. To date, a variety of 2D TMDCs have been shown for PL based sensing including TiS_2, TaS_2, WS_2, and MoS_2.[45,100] Many of these systems are based on the suspensions of 2D TMDCs that show PL when their lateral dimensions are reduced in size (specially the metallic 2D TMDCs that in natural state don't show any PL).

Plasmonics of 2D TMDCs can also be used for biosensing and therapeutics. However, due to the low carrier concentration of intrinsic semiconducting 2D TMDCs, plasmon resonances appear in THz.[101] Processes such as intercalation[102] or inducing defects and metallic edges[103] can be used for shifting these plasmon resonances to visible and IR optical ranges.

Effective optical sensing can be achieved by indirect reversible fluorescence quenching/enhancing that occurs when fluorescently tagged biomolecules, such as DNA or aptamers, are immobilised on the large surface area of 2D TMDCs.[38,104] Intercalations of H^+ or alkali ions can also render 2D semiconducting TMDCs metallic, quenching their PL. This concept has been applied to sense blood glucose based on the peroxidase-like activity of 2D MoS_2[17] and WS_2[14] flakes.

2D TMDCs can sense different gas species, including biologically important gas molecules such as NO,[105] NO_2,[106] or NH_3[13] and organic vapors.[107,108] The sensitivity of such 2D MoS_2 sensors can also be tuned by the functionalization with various components such as thiol containing chemicals.[109]

Composites with other components such as inorganic nanoparticles, graphene, carbon nanotubes and a number of polymers[11,16,110–114] have also been used for biosensing applications. These combinations offer the advantages of the conjugated materials, synergies, incorporated junction effects as well as enhanced sensitivity and selectivity.

2D TMDCs are also known to have an exceptional strain limit[115] and a high elastic modulus,[116,117] allowing the use in mechanical based bio transducers.[117] Recently, strong piezoelectric properties have been observed for single layered MoS_2, properties that do not exist for the bulk crystal.[33] The properties of single layers can be potentially employed to develop highly sensitive cantilever based mass detectors for biological molecules.

12. Other Applications

Biological applications are not limited to the aforementioned systems. 2D TMDCs have found promising applications in microbial electrolysis cells, reducing the overpotential for hydrogen gas production in order to achieve more efficient systems.[118,119] They have been used for sensing applications as flexible thin-film transistors.[120] 2D MoS_2 has been implemented for assessing cell viabilities based on exchanged alkali ions via protein nanopores embedded in cells' lipid bilayers,[17] a process which is empowered by the intrinsic voltage across such nanopores. They have also been implemented in realising DNA-origami concepts.[121] Another application is in DNA sequencing, where nanopores formed in 2D TMDCs offer a signal-to-noise ratio almost one order of magnitude superior to that of graphene.[9,122] Additionally, 2D TMDCs can be potentially used as substrates for immobilising live cells. TMDCs such as $MoTe_2$ offer high electron transfer possibilities that allow effective applications in tunnelling microscopy.[123,124] With the advent of force and tunnelling microscopy systems, which can operate efficiently in liquid media, such systems are poised to be more accessible for fundamental research revealing living cell activities.

13. Conclusions and Outlook

The application of 2D TMDCs in biological systems has gained rapid momentum in recent years. The properties of 2D TMDCs have shown distinct advantages for bio imaging and cell labelling, drug delivery and therapeutic applications, tissue engineering and biosensing. Yet these areas are still in their infancy, many opportunities are just emerging and significant advances are expected in the near future.

New areas of biology may yet benefit from the properties of 2D TMDCs. The ability to receive or transfer signals from living systems makes these materials particularly useful for probing cells. 2D TMDCs offer a variety of electronic structures allowing the development of flat materials ranging from near insulating to highly conductive. After their uptake into or being incubated onto cells, they can respond to external stimuli,

 i) Measurement of FRET pairing onto blue luminescent monolayered quasi 2D MoS_2 nanosheets and Alexa Fluor 430 commercial dye attached to single stranded DNA. On hybridisation of the DNA, these probes are separated by the length of the double stranded DNA. Alexa Fluor 430 is chosen as its adsorption at 430 nm overlaps with the PL emission wavelength of quasi 2D MoS_2 flakes (415 nm). So in the FRET pair, the MoS_2 and Alexa Fluor 430 could serve as a donor and an acceptor, respectively. Graph shows PL spectra of the MoS_2 and the Alexa Fluor 430 in the Alexa Fluor 430-double stranded DNA-MoS_2 conjugates when excited at 300 nm. Inset: the average PL intensities of the MoS_2 at 415 nm and the Alexa Fluor 430 at 530 nm depending on the donor–acceptor distance controlled by the number of base pairs. Reproduced with permission.[10]

altering and perturbing cells and/or their organelles. Their electron mobility and electron transfer to biological systems can be significantly adjusted via different linkers' lengths. 2D TMDCs can be readily affected by external electric and optical fields, so they can be potentially used for tissue engineering along the field lines.

The thermal properties of TMDCs include large along the plane thermal conductivities and thermoelectric coefficients, which can be employed for biosensing utilising templates that implement the planar structures or used for cooling or heating of cells and tissues.

Electrical and optical properties coupled with the atomic smoothness of TMDCs' surface should also allow exploratory atomic force microscopy of biological systems in liquid media. Intercalation can be used for creating planar structures that allow drug transfer along the plane with pore dimensions that can be as small as the adjustable spacing between two mono layers.

Biosensing, tissue engineering and drug encapsulations may be advanced by the investigations of composites containing 2D TMDCs together with both conductive and non-conductive polymers with a variety of organic and inorganic compounds. Conjugated polymers may play a pivotal role in designing such compounds due to their intrinsic electric conductivities. The prismatic edges of semiconducting 2D TMDCs could be functionalized to create rigid and yet light-weight structures for tissue engineering. Additionally, more investigations are required to gain deeper knowledge about the functionalization techniques for metallic 2D TMDCs.

The enzymatic activities, the capacity for intercalation and the potential differences between 2D TMDC and proteins or other biomolecules should be fully exploited. An important concept which will certainly play a role in the further expansion of the 2D TMDCs based biosensors is their incorporation with microfluidics, allowing their usage for point-of-care applications.

The synthetic routes used for producing 2D TMDCs offer many opportunities. 2D TMDC nanoflakes can be made of predetermined lateral dimensions to control both PL behavior and cellular uptake. More concerted efforts are required to develop green synthesis and intercalation techniques for 2D TMDCs that can be adopted and incorporated into the biosystems of choice. Additionally, highly sensitive biosensors, in nm dimensions, may also be constructed by electron/ion beam lithography, creating arrays of homogenous islands of 2D TMDCs on various substrates. These arrays can be designed to allow resonance and hence enhancement of localised PL or plasmonic peaks that can be potentially used in sensors for the detection of single bio molecules.

Synergetic effects between 2D TMDCs and other 2D materials including graphene and graphene analogues should also be further explored for biomedical applications.[97] These materials can be hold together via van der Waals forces, while each 2D component provides a unique physiochemical property that can be used for designing new compounds with extraordinary properties.

Versatility, controllability, and relatively high bio compatibility of 2D TMDCs will provide strong motivation for tailored expansion of these materials in biological systems. Undoubtedly, the key factor for successful research in relevant bio 2D TMDC areas will be the substantial and close interactions between researchers from different disciplines.

Acknowledgements

K.K. and T.D. acknowledge support from the Australian Research Council Discovery program (DP140100170). M.P. acknowledges a Tier 2 grant (MOE2013-T2–1–056) from Ministry of Education, Singapore.

Received: March 6, 2015
Revised: May 5, 2015
Published online: July 14, 2015

[1] D. Jariwala, V. K. Sangwan, L. J. Lauhon, T. J. Marks, M. C. Hersam, *ACS Nano* **2014**, *8*, 1102.
[2] S. Balendhran, S. Walia, H. Nili, J. Z. Ou, S. Zhuiykov, R. B. Kaner, S. Sriram, M. Bhaskaran, K. Kalantar-zadeh, *Adv. Funct. Mater.* **2013**, *23*, 3952.
[3] K. Mak, C. Lee, J. Hone, J. Shan, T. Heinz, *Phys. Rev. B* **2010**, *105*, 136805.
[4] Q. H. Wang, K. Kalantar-Zadeh, A. Kis, J. N. Coleman, M. S. Strano, *Nat. Nanotechnol.* **2012**, *7*, 699.
[5] R. Lv, J. A. Robinson, R. E. Schaak, D. Sun, Y. Sun, T. E. Mallouk, M. Terrones, *Acc. Chem. Res.* **2015**, *48*, 56.
[6] B. Radisavljevic, A. Radenovic, J. Brivio, V. Giacometti, A. Kis, *Nat. Nanotechnol.* **2011**, *6*, 147.
[7] M. Chhowalla, H. S. Shin, G. Eda, L.-J. Li, K. P. Loh, H. Zhang, *Nat. Chem.* **2013**, *5*, 263.
[8] S. Z. Butler, S. M. Hollen, L. Cao, Y. Cui, J. A. Gupta, H. R. Gutiérrez, T. F. Heinz, S. S. Hong, J. Huang, A. F. Ismach, E. Johnston-Halperin, M. Kuno, V. V. Plashnitsa, R. D. Robinson, R. S. Ruoff, S. Salahuddin, J. Shan, L. Shi, M. G. Spencer, M. Terrones, W. Windl, J. E. Goldberger, *ACS Nano* **2013**, *7*, 2898.
[9] A. B. Farimani, K. Min, N. R. Aluru, *ACS Nano* **2014**, *8*, 7914.
[10] H. D. Ha, D. J. Han, J. S. Choi, M. Park, T. S. Seo, *Small* **2014**, *10*, 3858.
[11] K.-J. Huang, Y.-J. Liu, H.-B. Wang, Y.-Y. Wang, Y.-M. Liu, *Biosens. Bioelectron.* **2014**, *55*, 195.
[12] G. Lalwani, A. M. Henslee, B. Farshid, L. Lin, F. K. Kasper, Y.-X. Qin, A. G. Mikos, B. Sitharaman, *Biomacromolecules* **2013**, *14*, 900.
[13] D. J. Late, Y.-K. Huang, B. Liu, J. Acharya, S. N. Shirodkar, J. Luo, A. Yan, D. Charles, U. V. Waghmare, V. P. Dravid, C. N. R. Rao, *ACS Nano* **2013**, *7*, 4879.
[14] T. Lin, L. Zhong, Z. Song, L. Guo, H. Wu, Q. Guo, Y. Chen, F. Fu, G. Chen, *Biosens. Bioelectron.* **2014**, *62*, 302.
[15] T. Liu, C. Wang, X. Gu, H. Gong, L. Cheng, X. Shi, L. Feng, B. Sun, Z. Liu, *Adv. Mater.* **2014**, *26*, 3433.
[16] Y.-M. Liu, M. Zhou, Y.-Y. Liu, G.-F. Shi, J.-J. Zhang, J.-T. Cao, K.-J. Huang, Y.-H. Chen, *RSC Adv.* **2014**, *4*, 22888.
[17] J. Z. Ou, A. F. Chrimes, Y. Wang, S. Y. Tang, M. S. Strano, K. Kalantar-Zadeh, *Nano Lett.* **2014**, *14*, 857.
[18] L. Wang, Y. Wang, J. I. Wong, T. Palacios, J. Kong, H. Y. Yang, *Small* **2014**, *10*, 1101.
[19] N. Wang, F. Wei, Y. Qi, H. Li, X. Lu, G. Zhao, Q. Xu, *ACS Appl. Mater. Interfaces* **2014**, *6*, 19888.
[20] T. Wang, R. Zhu, J. Zhuo, Z. Zhu, Y. Shao, M. Li, *Anal. Chem.* **2014**, *86*, 12064.
[21] X. Yang, J. Li, T. Liang, C. Ma, Y. Zhang, H. Chen, N. Hanagata, H. Su, M. Xu, *Nanoscale* **2014**, *6*, 10126.

[22] V. Nicolosi, M. Chhowalla, M. G. Kanatzidis, M. S. Strano, J. N. Coleman, *Science* **2013**, *340*, 1226419.
[23] W. Zhao, R. M. Ribeiro, G. Eda, *Acc. Chem. Res.* **2015**, *48*, 91.
[24] R. H. Holm, P. Kennepohl, E. I. Solomon, *Chem. Rev.* **1996**, *96*, 2239.
[25] H. Li, Q. Zhang, C. C. R. Yap, B. K. Tay, T. H. T. Edwin, A. Olivier, D. Baillargeat, *Adv. Funct. Mater.* **2012**, *22*, 1385.
[26] Y. Wang, J. Z. Ou, S. Balendhran, A. F. Chrimes, M. Mortazavi, D. D. Yao, M. R. Field, K. Latham, V. Bansal, J. R. Friend, S. Zhuiykov, N. V. Medhekar, M. S. Strano, K. Kalantar-zadeh, *ACS Nano* **2013**, *7*, 10083.
[27] E. Stern, R. Wagner, F. J. Sigworth, R. Breaker, T. M. Fahmy, M. A. Reed, *Nano Lett.* **2007**, *7*, 3405.
[28] W. Z. Teo, E. L. K. Chng, Z. Sofer, M. Pumera, *Chem. Eur. J.* **2014**, *20*, 9627.
[29] M. S. Fuhrer, J. Hone, *Nat. Nanotechnol.* **2013**, *8*, 146.
[30] S. S. Chou, B. Kaehr, J. Kim, B. M. Foley, M. De, P. E. Hopkins, J. Huang, C. J. Brinker, V. P. Dravid, *Angew. Chem. Int. Ed.* **2013**, *125*, 4254.
[31] W. Yin, L. Yan, J. Yu, G. Tian, L. Zhou, X. Zheng, X. Zhang, Y. Yong, J. Li, Z. Gu, Y. Zhao, *ACS Nano* **2014**, *8*, 6922.
[32] L. Kou, A. Du, C. Chen, T. Frauenheim, *Nanoscale* **2014**, *6*, 5156.
[33] W. Wu, L. Wang, Y. Li, F. Zhang, L. Lin, S. Niu, D. Chenet, X. Zhang, Y. Hao, T. F. Heinz, J. Hone, Z. L. Wang, *Nature* **2014**, *514*, 470.
[34] A. Splendiani, L. Sun, Y. Zhang, T. Li, J. Kim, C.-Y. Chim, G. Galli, F. Wang, *Nano Lett.* **2010**, *10*, 1271.
[35] M. Y. Han, B. Özyilmaz, Y. Zhang, P. Kim, *Phys. Rev. Lett.* **2007**, *98*, 206805.
[36] Y. Zhang, T.-T. Tang, C. Girit, Z. Hao, M. C. Martin, A. Zettl, M. F. Crommie, Y. R. Shen, F. Wang, *Nature* **2009**, *459*, 820.
[37] D. Xiao, G.-B. Liu, W. Feng, X. Xu, W. Yao, *Phys. Rev. Lett.* **2012**, *108*, 196802.
[38] C. Zhu, Z. Zeng, H. Li, F. Li, C. Fan, H. Zhang, *J. Am. Chem. Soc.* **2013**, *135*, 5998.
[39] L. Cheng, J. Liu, X. Gu, H. Gong, X. Shi, T. Liu, C. Wang, X. Wang, G. Liu, H. Xing, W. Bu, B. Sun, Z. Liu, *Adv. Mater.* **2014**, *26*, 1886.
[40] C. Ataca, H. Şahin, S. Ciraci, *J. Phys. Chem. C* **2012**, *116*, 8983.
[41] F. A. Rasmussen, K. S. Thygesen, *J. Phys. Chem. C* **2015**, *119*, 13169.
[42] A. K. Singh, K. Mathew, H. L. Zhuang, R. G. Hennig, *J. Phys. Chem. Lett.* **2015**, *6*, 1087.
[43] S. Lebègue, T. Björkman, M. Klintenberg, R. M. Nieminen, O. Eriksson, *Phys. Rev. X* **2013**, *3*, 031002.
[44] K. S. Novoselov, A. K. Geim, S. V. Morozov, D. Jiang, M. I. Katsnelson, I. V. Grigorieva, S. V. Dubonos, A. A. Firsov, *Nature* **2005**, *438*, 197.
[45] Y. Zhang, B. Zheng, C. Zhu, X. Zhang, C. Tan, H. Li, B. Chen, J. Yang, J. Chen, Y. Huang, L. Wang, H. Zhang, *Adv. Mater.* **2015**, *27*, 935.
[46] A. C. Ferrari, J. C. Meyer, V. Scardaci, C. Casiraghi, M. Lazzeri, F. Mauri, S. Piscanec, D. Jiang, K. S. Novoselov, S. Roth, A. K. Geim, *Phys. Rev. Lett.* **2006**, *97*, 187401.
[47] K. S. Novoselov, D. Jiang, F. Schedin, T. J. Booth, V. V. Khotkevich, S. V. Morozov, A. K. Geim, *Proc. Natl. Acad. Sci. U.S.A.* **2005**, *102*, 10451.
[48] K.-K. Liu, W. Zhang, Y.-H. Lee, Y.-C. Lin, M.-T. Chang, C.-Y. Su, C.-S. Chang, H. Li, Y. Shi, H. Zhang, C.-S. Lai, L.-J. Li, *Nano Lett.* **2012**, *12*, 1538.
[49] Y. Zhan, Z. Liu, S. Najmaei, P. M. Ajayan, J. Lou, *Small* **2012**, *8*, 966.
[50] T. Weber, J. C. Muijsers, J. H. M. C. van Wolput, C. P. J. Verhagen, J. W. Niemantsverdriet, *J. Phys. Chem.* **1996**, *100*, 14144.
[51] S. Balendhran, J. Z. Ou, M. Bhaskaran, S. Sriram, S. Ippolito, Z. Vasic, E. Kats, S. Bhargava, S. Zhuiykov, K. Kalantar-Zadeh, *Nanoscale* **2012**, *4*, 461.
[52] E. Benavente, M. A. Santa Ana, F. Mendizábal, G. González, *Coordin. Chem. Rev.* **2002**, *224*, 87.
[53] Z. Zeng, Z. Yin, X. Huang, H. Li, Q. He, G. Lu, F. Boey, H. Zhang, *Angew. Chem. Int. Ed.* **2011**, *50*, 11093.
[54] A. O'Neill, U. Khan, J. N. Coleman, *Chem. Mater.* **2012**, *24*, 2414.
[55] J. N. Coleman, M. Lotya, A. O'Neill, S. D. Bergin, P. J. King, U. Khan, K. Young, A. Gaucher, S. De, R. J. Smith, I. V. Shvets, S. K. Arora, G. Stanton, H. Y. Kim, K. Lee, G. T. Kim, G. S. Duesberg, T. Hallam, J. J. Boland, J. J. Wang, J. F. Donegan, J. C. Grunlan, G. Moriarty, A. Shmeliov, R. J. Nicholls, J. M. Perkins, E. M. Grieveson, K. Theuwissen, D. W. McComb, P. D. Nellist, V. Nicolosi, *Science* **2011**, *331*, 568.
[56] R. J. Smith, P. J. King, M. Lotya, C. Wirtz, U. Khan, S. De, A. O'Neill, G. S. Duesberg, J. C. Grunlan, G. Moriarty, J. Chen, J. Wang, A. I. Minett, V. Nicolosi, J. N. Coleman, *Adv. Mater.* **2011**, *23*, 3944.
[57] G. Guan, S. Zhang, S. Liu, Y. Cai, M. Low, C. P. Teng, I. Y. Phang, Y. Cheng, K. L. Duei, B. M. Srinivasan, Y. Zheng, Y.-W. Zhang, M.-Y. Han, *J. Am. Chem. Soc.* **2015**.
[58] B. J. Carey, T. Daeneke, E. P. Nguyen, Y. Wang, J. Zhen Ou, S. Zhuiykov, K. Kalantar-zadeh, *Chem. Commun.* **2015**, *51*, 3770.
[59] E. P. Nguyen, B. J. Carey, T. Daeneke, J. Z. Ou, K. Latham, S. Zhuiykov, K. Kalantar-zadeh, *Chem. Mater.* **2014**, *27*, 53.
[60] X. Yu, M. S. Prévot, K. Sivula, *Chem. Mater.* **2014**, *26*, 5892.
[61] C. Ataca, S. Ciraci, *J. Phys. Chem. C* **2011**, *115*, 13303.
[62] D. Voiry, A. Goswami, R. Kappera, e. SilvaCecilia de Carvalho Castro, D. Kaplan, T. Fujita, M. Chen, T. Asefa, M. Chhowalla, *Nat. Chem.* **2015**, *7*, 45.
[63] G. Eda, T. Fujita, H. Yamaguchi, D. Voiry, M. Chen, M. Chhowalla, *ACS Nano* **2012**, *6*, 7311.
[64] S. Najmaei, J. Yuan, J. Zhang, P. Ajayan, J. Lou, *Acc. Chem. Res.* **2015**, *48*, 31.
[65] S. S. Chou, M. De, J. Kim, S. Byun, C. Dykstra, J. Yu, J. Huang, V. P. Dravid, *J. Am. Chem. Soc.* **2013**, *135*, 4584.
[66] S. E. Moore, J. H. Lunsford, *J. Catal.* **1982**, *77*, 297.
[67] R. Coehoorn, C. Haas, J. Dijkstra, C. Flipse, R. de Groot, A. Wold, *Phys. Rev. B* **1987**, *35*, 6195.
[68] S. Jeong, D. Yoo, M. Ahn, P. Miró, T. Heine, J. Cheon, *Nat. Commun.* **2015**, *6*, 5763.
[69] T. Stephenson, Z. Li, B. Olsen, D. Mitlin, *Energ. Environ. Sci.* **2014**, *7*, 209.
[70] R. Bhandavat, L. David, G. Singh, *J. Phys. Chem. Lett.* **2012**, *3*, 1523.
[71] E. Benavente, G. González, *Mater. Res. Bull.* **1997**, *32*, 709.
[72] M. A. Lukowski, A. S. Daniel, C. R. English, F. Meng, A. Forticaux, R. J. Hamers, S. Jin, *Energ. Environ. Sci.* **2014**, *7*, 2608.
[73] R. Bissessur, J. L. Schindler, C. R. Kannewurf, M. Kanatzidis, *Mol. Cryst. Liq. Crys. A* **1994**, *245*, 249.
[74] J. P. Lemmon, J. Wu, C. Oriakhi, M. M. Lerner, *Electrochim. Acta* **1995**, *40*, 2245.
[75] V. Sánchez, E. Benavente, M. A. Santa Ana, G. González, *Chem. Mater.* **1999**, *11*, 2296.
[76] C. Backes, R. J. Smith, N. McEvoy, N. C. Berner, D. McCloskey, H. C. Nerl, A. O'Neill, P. J. King, T. Higgins, D. Hanlon, N. Scheuschner, J. Maultzsch, L. Houben, G. S. Duesberg, J. F. Donegan, V. Nicolosi, J. N. Coleman, *Nat. Commun.* **2014**, *5*, 4576.
[77] R. Anbazhagan, H. J. Wang, H. C. Tsai, R. J. Jeng, *RSC Adv.* **2014**, *4*, 42936.
[78] J.-M. Oh, T. T. Biswick, J.-H. Choy, *J. Mater. Chem.* **2009**, *19*, 2553.
[79] E. L. K. Chng, M. Pumera, *RSC Adv.* **2015**, *5*, 3074.
[80] E. L. K. Chng, Z. Sofer, M. Pumera, *Nanoscale* **2014**, *6*, 14412.
[81] I. Corazzari, F. Deorsola, G. Gulino, E. Aldieri, S. Bensaid, F. Turci, D. Fino, *J. Nanopart. Res.* **2014**, *16*, 1.
[82] S. Liu, T. H. Zeng, M. Hofmann, E. Burcombe, J. Wei, R. Jiang, J. Kong, Y. Chen, *ACS Nano* **2011**, *5*, 6971.

[83] X. Qian, S. Shen, T. Liu, L. Cheng, Z. Liu, *Nanoscale* **2015**, *7*, 6380.
[84] B. Tian, C. Wang, S. Zhang, L. Feng, Z. Liu, *ACS Nano* **2011**, *5*, 7000.
[85] K. Yang, S. Zhang, G. Zhang, X. Sun, S.-T. Lee, Z. Liu, *Nano Lett.* **2010**, *10*, 3318.
[86] Y. Yong, L. Zhou, Z. Gu, L. Yan, G. Tian, X. Zheng, X. Liu, X. Zhang, J. Shi, W. Cong, W. Yin, Y. Zhao, *Nanoscale* **2014**, *6*, 10394.
[87] Z. Sheng, L. Song, J. Zheng, D. Hu, M. He, M. Zheng, G. Gao, P. Gong, P. Zhang, Y. Ma, L. Cai, *Biomaterials* **2013**, *34*, 5236.
[88] T. Liu, S. Shi, C. Liang, S. Shen, L. Cheng, C. Wang, X. Song, S. Goel, T. E. Barnhart, W. Cai, Z. Liu, *ACS Nano* **2015**, *9*, 950.
[89] S. Xu, D. Li, P. Wu, *Adv. Funct. Mater.* **2015**, *25*, 1127.
[90] P. M. Ajayan, J. M. Tour, *Nature* **2007**, *447*, 1066.
[91] D. Sarkar, W. Liu, X. Xie, A. C. Anselmo, S. Mitragotri, K. Banerjee, *ACS Nano* **2014**, *8*, 3992.
[92] T. Kuila, S. Bose, P. Khanra, A. K. Mishra, N. H. Kim, J. H. Lee, *Biosens. Bioelectron.* **2011**, *26*, 4637.
[93] S. Wu, Z. Zeng, Q. He, Z. Wang, S. J. Wang, Y. Du, Z. Yin, X. Sun, W. Chen, H. Zhang, *Small* **2012**, *8*, 2264.
[94] A. H. Loo, A. Bonanni, A. Ambrosi, M. Pumera, *Nanoscale* **2014**, *6*, 11971.
[95] T. Wang, H. Zhu, J. Zhuo, Z. Zhu, P. Papakonstantinou, G. Lubarsky, J. Lin, M. Li, *Anal. Chem.* **2013**, *85*, 10289.
[96] G.-X. Wang, W.-J. Bao, J. Wang, Q.-Q. Lu, X.-H. Xia, *Electrochem. Commun.* **2013**, *35*, 146.
[97] Y. Chen, C. Tan, H. Zhang, L. Wang, *Chem. Soc. Rev.* **2015**, *44*, 2681–2701.
[98] H. Fang, S. Chuang, T. C. Chang, K. Takei, T. Takahashi, A. Javey, *Nano Lett.* **2012**, *12*, 3788.
[99] Y. Wang, Y. Ni, *Anal. Chem.* **2014**, *86*, 7463.
[100] Y. Yuan, R. Li, Z. Liu, *Anal. Chem.* **2014**, *86*, 3610.
[101] A. Scholz, T. Stauber, J. Schliemann, *Phys. Rev. B* **2013**, *88*, 035135.
[102] Y. Wang, J. Z. Ou, A. F. Chrimes, B. J. Carey, T. Daeneke, M. M. Y. A. Alsaif, M. Mortazavi, S. Zhuiykov, N. Medhekar, M. Bhaskaran, J. R. Friend, M. S. Strano, K. Kalantar-Zadeh, *Nano Lett.* **2015**, *15*, 883.
[103] K. Andersen, K. W. Jacobsen, K. S. Thygesen, *Phys. Rev. B* **2014**, *90*, 161410.
[104] J. Ge, E.-C. Ou, R.-Q. Yu, X. Chu, *J. Mater. Chem. B* **2014**, *2*, 625.
[105] H. Li, Z. Yin, Q. He, H. Li, X. Huang, G. Lu, D. W. H. Fam, A. I. Y. Tok, Q. Zhang, H. Zhang, *Small* **2012**, *8*, 63.
[106] Q. Yue, Z. Shao, S. Chang, J. Li, *Nanoscale Res Lett* **2013**, *8*, 1.
[107] N. Huo, S. Yang, Z. Wei, S.-S. Li, J.-B. Xia, J. Li, *Sci. Rep.* **2014**, *4*, 5209.
[108] F. K. Perkins, A. L. Friedman, E. Cobas, P. M. Campbell, G. G. Jernigan, B. T. Jonker, *Nano Lett.* **2013**, *13*, 668.
[109] J.-S. Kim, H.-W. Yoo, H. O. Choi, H.-T. Jung, *Nano Lett.* **2014**, *14*, 5941.
[110] S. Su, H. Sun, F. Xu, L. Yuwen, L. Wang, *Electroanalysis* **2013**, *25*, 2523.
[111] J. Huang, Z. Dong, Y. Li, J. Li, W. Tang, H. Yang, J. Wang, Y. Bao, J. Jin, R. Li, *Mater. Res. Bull.* **2013**, *48*, 4544.
[112] K.-J. Huang, L. Wang, J. Li, Y.-M. Liu, *Sens. Actuators, B* **2013**, *178*, 671.
[113] Q. Feng, K. Duan, X. Ye, D. Lu, Y. Du, C. Wang, *Sens. Actuators, B* **2014**, *192*, 1.
[114] C. Tan, H. Zhang, *Chem. Soc. Rev.* **2015**, *44*, 2713–2731.
[115] K. He, C. Poole, K. F. Mak, J. Shan, *Nano Lett.* **2013**, *13*, 2931.
[116] A. Castellanos-Gomez, M. Poot, G. A. Steele, H. S. J. van der Zant, N. Agraït, G. Rubio-Bollinger, *Adv. Mater.* **2012**, *24*, 772.
[117] A. Castellanos-Gomez, R. van Leeuwen, M. Buscema, H. S. J. van der Zant, G. A. Steele, W. J. Venstra, *Adv. Mater.* **2013**, *25*, 6719.
[118] B. Hinnemann, P. G. Moses, J. Bonde, K. P. Jørgensen, J. H. Nielsen, S. Horch, I. Chorkendorff, J. K. Nørskov, *J. Am. Chem. Soc.* **2005**, *127*, 5308.
[119] J. C. Tokash, B. E. Logan, *Int. J. Hydrogen Energy* **2011**, *36*, 9439.
[120] Q. He, Z. Zeng, Z. Yin, H. Li, S. Wu, X. Huang, H. Zhang, *Small* **2012**, *8*, 2994.
[121] X. Zhang, M. Rahman, D. Neff, M. L. Norton, *Beilstein J. Nanotechnol.* **2014**, *5*, 501.
[122] K. Liu, J. Feng, A. Kis, A. Radenovic, *ACS Nano* **2014**, *8*, 2504.
[123] H. Jungblut, S. A. Campbell, M. Giersig, D. J. Muller, H. J. Lewerenz, *Farad. Discuss.* **1992**, *94*, 183.
[124] H. J. Lewerenz, *Phys. Status Solidi* **2008**, *245*, 1884.
[125] A. Kuc, N. Zibouche, T. Heine, *Phys. Rev. B* **2011**, *83*, 245213.